From data to theory and back
Detector geometry and data analysis

Riccardo Sturani

August 3rd, 2015

1 GW basics

We know that the GWs $\bar{h}_{\mu\nu} \equiv h_{\mu\nu} - 1/2\eta_{\mu\nu}h$ satisfy the wave equation in vacuum

$$\Box\bar{h}_{\mu\nu} = 0 \tag{1}$$

which holds in the gauge

$$\partial^\mu \bar{h}_{\mu\nu} = 0\,. \tag{2}$$

However the description in terms of a 10-component tensor is still redundant. We can use the diffeomorphism invariance $x^\mu \to x'^\mu + \xi^\mu$ acting on the metric perturbation as

$$h_{\mu\nu} \to h'_{\mu\nu} = h_{\mu\nu} + \xi_{\mu,\nu} + \xi_{\nu,\mu} \tag{3}$$

to isolate the physical, radiative degrees of freedom by observing that a diffeormophism preserving the gauge condition (2) satisfies the *Lorentz condition*

$$\Box\xi^\mu = 0\,. \tag{4}$$

As long as eq. (4) is satisfied we can then perform a gauge transformation to set to 0 some components of $\bar{h}_{\mu\nu}$. Note that this would *not be possible* if $T_{\mu\nu} \neq 0$ (it would appear on the right hand side of eq. (1)), as ξ^μ and $\bar{h}_{\mu\nu}$ would then satisfy different equations.

Let us thus choose a specific ξ^μ to impose 4 conditions on $\bar{h}_{\mu\nu}$. In particular $\bar{h} \to \bar{h}' = \bar{h} + \xi_\mu{}^{;\mu}$ so one can choose ξ_0, say, to set $\bar{h} = 0$, hence $\bar{h}_{\mu\nu} = h_{\mu\nu}$. The 3 ξ^is can be chose to make $h'_{0i} = h_{0i} + \xi_{i,0} + \xi_{0,i} = 0$ hence the 0-component of the Lorentz condition (2) becomes

$$-\dot{h}_{00} + h_{0i}{}^{;i} = 0\,, \tag{5}$$

but since h_{0i} have been made vanish this implies that h_{00} is time-independent, so it can be discarded as it cannot parametrize any radiative degree of freedom. Summarizing we have the 8 conditions

$$h_{0\mu} = 0\,, \qquad h^i_i = 0\,, \qquad h_{ij}{}^{;j} = 0 \tag{6}$$

defining the *transverse-traceless (TT)* gauge. The 2 radiative degrees of freedom of the TT gauge can be parametrized by

$$h_{ij}^{TT}(t,x) = \int \frac{d^3k}{(2\pi)^3} A_{ij}(\omega) e^{i(\omega t - \mathbf{kx})} \tag{7}$$

with $\omega = |\mathbf{k}|$, $\mathbf{k} = \omega\hat{\mathbf{n}}$ (we use $c = 1$ units) and the A_{ij} tensor can have only 2 independent non-vanishing components, that for a wave propagating in the z-direction (hence with $e_{iz} = 0$) can be written as

$$A_{ij}(\hat{\mathbf{z}}) = \begin{pmatrix} h_+ & h_\times & 0 \\ h_\times & -h_+ & 0 \\ 0 & 0 & 0 \end{pmatrix} \tag{8}$$

A convenient way to obtain the TT part of a tensor is to apply the projection tensor

$$\begin{array}{lcl} \Lambda_{ij,kl}(\hat{\mathbf{n}}) & \equiv & P_{ik}P_{jl} - \frac{1}{2}P_{ij}P_{kl}\,, \\ P_{ij}(\hat{\mathbf{n}}) & \equiv & \delta_{ij} - n_i n_j\,. \end{array} \tag{9}$$

A wave propagating along the generic direction $\hat{\mathbf{n}}$ can be obtained from eq. (8) by

$$A_{ij}(\hat{\mathbf{n}}) = R^{(z)}_{ii'}(\phi) R^{(y)}_{i'i''} e_{i''j''}(\hat{\mathbf{z}}) (R^{(y)})^{-1}_{j''j'}(\theta) (R^{(z)})^{-1}_{j'j}(\phi) \tag{10}$$

with

$$R^{(z)}(\phi) = \begin{pmatrix} \cos\phi & \sin\phi & 0 \\ -\sin\phi & \cos\phi & 0 \\ 0 & 0 & 1 \end{pmatrix} \tag{11}$$

$$R^{(y)}(\theta) = \begin{pmatrix} \cos\theta & 0 & \sin\theta \\ 0 & 1 & 0 \\ -\sin\theta & 0 & \cos\theta \end{pmatrix} \tag{12}$$

yielding to

$$\begin{array}{lcl} A_{xx}(\hat{\mathbf{n}}) & = & h_+\left(\cos^2\theta\cos^2\phi - \sin^2\phi\right) + 2h_\times\cos\theta\sin\phi\cos\phi\,, \\ A_{yy}(\hat{\mathbf{n}}) & = & h_+\left(\cos^2\theta\sin^2\phi - \cos^2\phi\right) - 2h_\times\cos\theta\sin\phi\cos\phi\,. \end{array} \tag{13}$$

For generic direction propagation it is also convenient to express the tensor e_{ij} in terms of 2 orthogonal unit vectors $\hat{\mathbf{u}}$ and $\hat{\mathbf{v}}$ spanning the plane orthogonal to the propagation direction, so that $\hat{\mathbf{n}} \times \hat{\mathbf{u}} = \hat{\mathbf{v}}$ and $A_{ij} = e^+_{ij}h_+ + e^\times_{ij}h_\times$ with

$$\begin{array}{l} e^+_{ij}(\hat{\mathbf{n}}) = \hat{\mathbf{u}}_i\hat{\mathbf{u}}_j - \hat{\mathbf{v}}_i\hat{\mathbf{v}}_j \\ e^\times_{ij}(\hat{\mathbf{n}}) = \hat{\mathbf{u}}_i\hat{\mathbf{v}}_j + \hat{\mathbf{v}}_i\hat{\mathbf{u}}_j \end{array} \tag{14}$$

We'll see in the next section that this are the only two components we need for an interferometer.

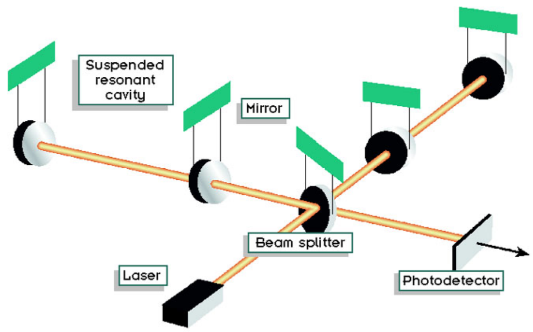

Figure 1: Interferometer scheme. Light emitted from the laser is shared by the two orthogonal arms after going through the beam splitter. After bouncing at the end mirrors it is recombined at the photo-detector.

2 Interaction detector - GWs

The arrival of a gravitational wave (GW) onto a detector will in general alter the state of motion of an observer and the goal of this section is to study the energy exchange of a GW with the laser interferometer components: beam splitter, end mirrors and the laser itself. Let us place them in the $z = 0$ plane at coordinates respectively $(0, 0)$, $(L_x, 0)$ and $(0, L_y)$ and consider for simplicity a GW traveling along the z direction. In the Transverse-Traceless (TT) gauge the gravitational perturbation $h_{\mu\nu}$ has components $h_{0\mu} = 0$, $h_{xx} = -h_{yy} = h_+$, $h_{xy} = h_{yx} = h_\times$, and the the metric element restricted to the x-y plane can be written as

$$d\tau^2\big|_{z=0} = dt^2 - (1 + h_+)dx^2 - (1 - h_+)dy^2 - 2(1 + h_\times)dxdy\,. \qquad (15)$$

Interaction between the GW and matter Given two nearby geodesic parametrized by coordinates $x^i(\tau), x'^i(\tau)$, describing the motion of two test masses initially at rest ($dx^i/d\tau|_{\tau=0} = 0 = dx'^i/d\tau|_{\tau=0}$, $dt/d\tau|_{\tau=0} = 1 = dt'/d\tau|_{\tau=0}$), the (space) *coordinate* geodesic deviation $\xi^i \equiv x'^i - x^i$ at initial time satisfies (see sec. 1.3 of [4])

$$\left.\frac{d^2\xi}{d\tau^2}\right|_{\tau=0} = -\dot{h}_{ij}\left.\frac{d\xi^i}{d\tau}\right|_{\tau=0}\,, \qquad (16)$$

as in the TT gauge at linear order $\partial_\mu\Gamma^i_{00} = 0$ and $\Gamma^i_{0j} = \partial_0 h_{ij}/2$, showing that the *coordinate* distance of two particle initially at rest remain constants in the TT gauge under the influence of a GW. However the *proper* distance s between the x-mirror and the beam splitter changes:

$$s = L_x(1 + h_+)^{1/2} \simeq L_x\left(1 + \frac{1}{2}h_+\right)\,, \qquad (17)$$

whose second derivative gives a Newtonian-like equation of motion

$$\ddot{s} \simeq \frac{1}{2}\ddot{h}_+ L_x \simeq \frac{1}{2}\ddot{h}_+ s \tag{18}$$

as to lowest order in h, $s \simeq L_x$. As the physical distance between two test masses (like the mirror and the beam splitter) is time dependent in the presence of a GW, it is expected that an energy transfer may take place between the GW and the interferometer, as first suggested in [1], by "putting in a spring" between objects in mutual motion.

The mirror and the beam splitter are hung to the ceiling of the laboratory, in a pendulum-like arrangement. The pendulum has a typical restoring period $T \sim \sqrt{l/g} \simeq$ few $\times 10^{-1}$ sec (being l the length of the suspension and g the gravity acceleration), implying that the mirror is approximately in free fall for GW signals whose frequency $f_{GW} \gg Hz$. On longer time scales energy transfer, and eventually dissipation, between the mirror and its suspension will take place.

In a real laboratory, positions are marked by rigid rulers and not by freely falling particles. It is thus instructive to consider the mirror-GW interaction in the *proper detector frame* (PDF). A standard results within General Relativity is that it always possible to set to zero the Christoffel symbols $\Gamma^{\rho}_{\mu\nu}$ along an entire geodesic by using Fermi normal coordinates in the freely falling frame, see sec. 8.4 of [2]. Considering the relative coordinate distance x^i between an arbitrary space-time point and to the geodesic used to define Fermi normal coordinates, to linear order in x the metric is flat and at second order in x/λ (being λ the curvature scale of the space-time, $\lambda \sim |R_{0i0j}|^{-1/2}$) one has in the proper detector frame

$$d\tau^2_{PDF} \simeq dt^2\left(1 + R_{0i0j}x^i x^j\right) + 2dt dx^i\left(\frac{2}{3}R_{0jik}x^j x^k\right) - dx^i dx^j\left(\delta_{ij} - \frac{1}{3}R_{ikjl}x^k x^l\right)\,. \tag{19}$$

The laboratory may not be in free fall with respect to earth gravity field, but if we restrict to motion in the $z = 0$ plane and to signals with $f_{GW} \gtrsim 10Hz$ all "environmental" effects can be safely neglected and the coordinate distance between neighboring geodesic results in

$$\ddot{\xi}^i_{PDF} = -R^i_{0j0}\xi^j_{PDF}\,. \tag{20}$$

Observing that at $O(x/\lambda)$ the metric is flat and that the Riemann tensor components are not only *covariant* (as common in General Relativity) but actually *invariant* in the linearized theory, so that $R^i_{0j0} = -\ddot{h}_{ij}/2$, being h the TT metric perturbation, we recover eq. (18), which is frame-independent. Since in the proper detector frame coordinates track distances, from eq. (18) we infer that a test particle of mass μ under the influence of a GW is experiencing a time-dependent, Newtonian force $F^i = -\frac{\mu}{2}\ddot{h}^{ij}L^j$, allowing to derive the energy-transfer rate dE/dt due to the force via $dE/dt = F^i dx^i/dt$.

In the presence of the GW only, $F^i dx^i/dt$ is a total derivative and for an oscillating h it averages to 0: after a short transient during which the massive object is set in motion by the GW there is no more energy transfer on average over an oscillation cycle. However the interferometer mirrors are not exactly freely-falling, because of the suspensions hanging them causes dissipation, leading to the actual equation (dropping the proper detector frame subscript)

$$\ddot{\xi}^i + \frac{\omega_0}{Q}\dot{\xi}^i + \omega_0^2 \xi^i = -\frac{1}{2}\ddot{h}_{ij}\xi^j \,, \tag{21}$$

with $\omega_0 = 2\pi/T$ the pendulum proper angular frequency and the ω_0/Q term parametrizing the friction term, for which we assume $Q \gg 1$. Assuming for simplicity a GW of the type $h_+ = h_0 \cos(\omega_{GW} t)$, $h_\times = 0$, we have the solution

$$\xi(t) - L = \left(2Lh_0\omega_{GW}^2/\pi^2\right) \frac{(\omega_{GW}^2 - \omega_0^2)\cos(\omega_{GW}t) - \omega_{GW}\omega_0/Q \sin(\omega_{GW}t)}{\left(\omega_{GW}^2 - \omega_0^2\right)^2 + \omega_{GW}^2\omega_0^2/Q^2} \,, \tag{22}$$

showing that the massive object motion is in phase with the GW, apart for a term proportional to the friction which is responsible for the dissipation

$$\left\langle \frac{dE}{dt} \right\rangle \simeq \left(\mu L^2 h_0^2 \omega_{GW}^8/\pi^4\right) \frac{(\omega_{GW}^2 - \omega_0^2)\omega_0/Q}{\left[\left(\omega_{GW}^2 - \omega_0^2\right)^2 + \omega_{GW}^2\omega_0^2/Q^2\right]^2} \,. \tag{23}$$

In the limit $\omega_{GW} \gg \omega_0$ one obtains

$$\begin{aligned} \frac{dE}{dt} \simeq \frac{\mu}{Q\pi^4} L^2 h_0^2 \omega_{GW}^2 \omega_0 \quad &\simeq 2\times 10^{12} h_0^2 \text{erg/sec} \\ &\times \left(\frac{Q}{10^8}\right)^{-1} \left(\frac{\omega_{GW}}{2\pi kHz}\right)^2 \left(\frac{\omega_0}{2\pi Hz}\right) \left(\frac{\mu}{1kg}\right) \left(\frac{L}{3km}\right)^2 , \end{aligned} \tag{24}$$

showing that the energy absorbed by the system from the GW is proportional to the friction term[1]. This is the energy absorbed by the massive object in order to keep its motion with a constant kinetic energy E_{kin} (averaged over a GW cycle)

$$\langle E_{kin} \rangle \simeq \mu \omega_{GW}^2 L^2 h_0^2/\pi^2 \,. \tag{25}$$

Interaction between the GW and and a Michelson-type interferometer. The laser in an interferometer monitors the distance between mirrors, and its electric field is also affected by the GW. The electric field in the two orthogonal beams in the interferometers "travel" from the beam splitter to the mirrors and back to recombine at the photo-detector at some time t. The phase of the electric field is conserved during free propagation, so at time t the electric fields

[1] In principle one could consider the re-emission by the system made by the beam-splitter and the mirror, which has a time-varying quadrupole $Q_{xx}(t) \simeq \mu\xi^2(t)$. From the standard Einstein quadrupole formula $dE/dt|_{emitted} = G_N \dddot{Q}_{ij}^2/5 \sim G_N \mu^2 L^4 \omega_{GW}^6 h_0^2$, which can be compared to the absorption given from eq. (24) to obtain
$dE/dt|_{emitted} \sim dE/dt|_{absorbed} \simeq 6\times 10^{-22} \left(\frac{\omega_0}{2\pi Hz}\right)^{-1} \left(\frac{\omega_{GW}}{2\pi kHz}\right)^4 \left(\frac{Q}{10^8}\right) \left(\frac{\mu}{1kg}\right) \left(\frac{L}{3km}\right)^2$,
hence completely negligible.

recombine with the phase they inherit from the times $t_0^{(x)} \neq t_0^{(y)}$ when they left the beam splitter. Denoting by $E^{(x)}$ and $E^{(y)}$ the electric field coming respectively from the x and y arms, once they are recombining at the photo-detector after the beam splitter, we have

$$\begin{aligned} E^{(x)} &= -\frac{1}{2} E_0 e^{-i\omega_l t_0^{(x)}} , \\ E^{(y)} &= \frac{1}{2} E_0 e^{-i\omega_l t_0^{(y)}} , \end{aligned} \tag{26}$$

with ω_l being the laser angular frequency and the relative minus sign is due to the fact that reflection from opposite sides of the beam splitter brings a π shift in the phase [3]. Using the null geodesic in the metric given by eq. (15) to relate the time t to $t_0^{(x,y)}$, we have (see sec. 9.1 of [4]) at $O(h)$

$$\begin{aligned} t_0^{(x)} &= t - 2L_x - h_+(t - L_x) \sin(\omega_{GW} L_x)/\omega_{GW} , \\ t_0^{(y)} &= t - 2L_y + h_+(t - L_y) \sin(\omega_{GW} L_y)/\omega_{GW} . \end{aligned} \tag{27}$$

Substituting the above expression for $t_0^{(x,y)}$ in eqs. (26) and expanding at linear order in the GW amplitude one obtains

$$\begin{aligned} E^{(x)}(t) = -\frac{1}{2} E_0 \quad & e^{i(2\omega_l L + \phi_0)} \left[e^{-i\omega_l t} + \frac{i}{2} h_0 \omega_l L \frac{\sin(\omega_{GW} L)}{\omega_{GW} L} \times \right. \\ & \left. \left(e^{-i(\omega_l - \omega_{GW})t} e^{-i\omega_{GW} L} + e^{-i(\omega_l + \omega_{GW})t} e^{i\omega_{GW} L} \right) \right] \end{aligned} \tag{28}$$

where we have introduced $L \equiv (L_x + L_y)/2$ and $\phi_0 \equiv \omega_l \Delta L$, with $\Delta L \equiv L_x - L_y$, and where in $O(h_0)$ terms we have identified $L_x \simeq L_y \simeq L$. This shows that in each arm *sidebands* appear beside the career laser frequency at angular frequencies $\omega_l \pm \omega_{GW}$. The relative amplitude of the sidebands with respect to the career laser signal, for $\omega_{GW} \ll 1/L$, is given approximately by $h_0 L/\lambda_l \gg h_0$, being λ_l the laser wavelength.
Combining eq. (28) with the analogous formula for the y-arm one can determine the total electric field at the photo-detector $E_{pd}(t) = E^{(x)} + E^{(y)}$

$$E_{pd} = -iE_0 e^{-i\omega_l (t-2L)} \sin \left[\phi_0 + h_0 \omega_l L \frac{\sin(\omega_{GW} L)}{\omega_{GW} L} \cos(\omega_{GW}(t - L)) \right] . \tag{29}$$

Detecting a GW from the laser light associated with this electric field is still impractical: in order for the output power be *linear* in h_0 one would be sensitive also to the fluctuations in the laser power at a frequency $\sim \omega_{GW}/(2\pi)$, that would completely hide the GW signal. The solution adopted in actual observatories is to inject sidebands into the laser light so that the input electric field is given by

$$\begin{aligned} E_{in} &= E_0 e^{-i(\omega_l t + \Gamma \sin(\Omega_{mod} t))} \\ &\simeq E_0 \left[e^{-i\omega_l t} + \frac{\Gamma}{2} e^{-i(\omega_l + \Omega_{mod})t} - \frac{\Gamma}{2} e^{-i(\omega_L - \Omega_{mod})t} \right] , \end{aligned} \tag{30}$$

Working with $\phi_0 = 0$, so that $E_{pd} \propto h_0$ as per eq. (29), and combining the effects of the GW with the injected modulating sidebands, one has the output electric field

$$\begin{aligned} E_{out} \simeq \quad & -iE_0 e^{-i(\omega_l t+2L)} \left[\omega_l L \frac{\sin(\omega_{GW} L)}{\omega_{GW} L} h_0 \cos(\omega_{GW} t) \right. \\ & \left. +2\Gamma \sin(\Omega_{mod}\Delta L) \cos(\Omega_{mod}(t-2L)) \right], \end{aligned} \tag{31}$$

and the GW signal can be read in the output power from the interference term between the career field and the sidebands oscillating at $\pm\Omega_{mod}$, giving a light power at the photo-detector P_{pd} (for $\omega_{GW} L \ll 1$)

$$P_{pd} = |E_{out}|^2 \simeq 2E_0^2 \Gamma \omega_l L h_0 \cos(\omega_{GW} t) \sin(\Omega_{mod}\Delta L) \sin(\Omega_{mod}(t-2L)) + \ldots \tag{32}$$

where only the term oscillating at $\pm\Omega_{mod} \pm \omega_{GW}$ has been explicitly shown, as it is the only one linear in the GW amplitude.
The output is still sensitive to the power fluctuation (of the sidebands), but now the GW signal has to compete with laser power fluctuation not at $\omega_{GW} \lesssim 10$ kHz, but at $\Omega_{mod} \sim 10$ MHz $\gg \omega_{GW}$ and this is a great advantage as laser power fluctuations generally decrease with frequency [6].

The interferometers actually used as GW observatories contain Fabry-Perot cavities in which the laser beam goes back and forth several times in each arm before recombining. At an effective level, the Fabry-Perot cavity allow to "fold" the light path enhancing its length without changing the region of the laboratory space traveled by the laser. This results in a phase-shift enhanced, in the case $\omega_{GW} L \gg 1$, by a factor $N \equiv 4F/\pi$ (see e.g. sec. 9.2 of [4]) where F is the *finesse* of the cavity related to the *storage time* (i.e. the average time spent by a photon in the cavity) τ_s by $F \simeq \pi\tau_s/L$: the effect of the Fabry-Perot cavity boils down to replace the term $h_0 L$ in the amplitude of the GW sidebands in eq. (28) with

$$h_0 N L \frac{1}{\left[1 + (N L \omega_{GW}/2)^2\right]^{1/2}}, \qquad \text{for } \omega_{GW} L \ll 1 \,. \tag{33}$$

For initial LIGO (Virgo) $N \simeq 60(20)$.

The laser electric fields recombines at the beam splitter to form an output beam directed to the photo-detector and a beam heading back to the laser. We have described how the electric field at the photo-detector depend on the GW in eq. (29). The electric field going back to the laser is $E_l = E^{(x)} - E^{(y)}$ (apart from an irrelevant overall phase), thus we can compute the total laser power

$$|E^{(x)} + E^{(y)}|^2 + |E^{(x)} - E^{(y)}|^2 = E_0^2 \,, \tag{34}$$

which is unaffected by the GW, at least at $O(h)$. The appearance of the GW sidebands does not change the total power in the laser beam, but allows to identify a signal at a well-determined frequency and with amplitude highly enhanced with respect to h_0, see the $\omega_l L$ factor in eq. (32).

In order to complete the energy balance of the interferometer interacting with a GW however we still need to consider the radiation pressure exerting a force F_{rp} on the masses set in motion by the GW [5]. The laser power in each arm is approximately $P_{arm} = P_{laser}/2 = E_0^2/2$ and the radiation-pressure induces a force on each end mirror $F_{rp} = 2P_{arm} = P_{laser}$. As the masses are set in motion by the GW with velocity v, the radiation pressure force change because of the Doppler effect to $F_{rp} \simeq 2P_{arm}(1-2v)$, where v can be obtained by deriving eq. (22). The radiation pressure force has thus the effect of a friction term of the kind appearing in eq. (21), with an effective "quality factor" Q_{rp} approximately given by

$$Q_{rp} = \frac{m\omega_0}{4P_{arm}} \simeq 3\times 10^{15}\left(\frac{P_{laser}}{100W}\right)^{-1}\left(\frac{m}{1kg}\right)\left(\frac{\omega_0}{1Hz}\right) . \qquad (35)$$

Summing over the repeated bounces of each photon in the Fabry-Perot cavity, one can derive the dissipation due to radiation pressure [5]

$$\left.\frac{dE}{dt}\right|_{rp} \simeq 4P_{arm}\frac{N^2L^2}{\pi^2}h_0^2\omega_{GW}^2 \qquad (36)$$

which can be obtained by substituting Q_{rp} in eq. (24) and replacing L with NL.

3 Detector geometry

We have seen in the previous section that an interferometer responds to the component combination $h_{xx} - h_{yy}$, which can be put into an invariant form by saying that the detector's output $o(t)$ is sensitive to the wave combination $D_{ij}h_{ij}$ with

$$D_{ij} = \frac{1}{2}\left(\hat{\mathbf{x}}_i\hat{\mathbf{x}}_j - \hat{\mathbf{y}}_i\hat{\mathbf{y}}_j\right) . \qquad (37)$$

Short-circuiting with the detector tensor D_{ij} with $e_{ij}(\hat{\mathbf{n}})$ computed in sec.1 one obtains the *pattern functions*, which relate the GW amplitude depending only on the source to its actual imprint in the detector.

By expressing $h(t)$ as

$$h(t) = D_{ij}h_{ij}^{TT}(t,\mathbf{x}_D) = D_{ij}e_{ij}^A(\hat{\mathbf{n}})h_A(t) \equiv F_+(\theta,\phi)h_+(t) + F_\times(\theta,\phi)h_\times(t) \qquad (38)$$

we have introduced the pattern functions F_A, with their explicit dependence on θ, ϕ, the angles determining the arrival direction $\hat{\mathbf{n}} = (\sin\theta\cos\phi, \sin\theta\sin\phi, \cos\theta)$. The choice of unit vectors $\hat{\mathbf{u}}, \hat{\mathbf{v}}$ is unique up to a rotation in the plane they span, that is choosing $\hat{\mathbf{u}}' = \hat{\mathbf{u}}\cos\psi - \hat{\mathbf{v}}\sin\psi$ and $\hat{\mathbf{v}}' = \hat{\mathbf{v}}\cos\psi + \hat{\mathbf{u}}\sin\psi$ one obtains different polarization tensors

$$\begin{aligned} e_{ij}^{+\prime} &= \hat{\mathbf{u}}_i'\hat{\mathbf{u}}_j' - \hat{\mathbf{v}}_i'\hat{\mathbf{v}}_j' = e_{ij}^+\cos 2\psi - e_{ij}^\times\sin 2\psi\,, \\ e_{ij}^{\times\prime} &= \hat{\mathbf{u}}_i'\hat{\mathbf{v}}_j' + \hat{\mathbf{v}}_i'\hat{\mathbf{u}}_j' = e_{ij}^+\sin 2\psi + e_{ij}^\times\cos 2\psi\,, \end{aligned} \qquad (39)$$

hence the patter functions obtained by contracting the polarization tensors with the detector tensor will transform as (with an abuse of notation we write with the same symbol the pattern functions and their transformed under a rotation depending on the extra variable ψ)

$$\begin{array}{l} F'_+(\theta,\phi,\psi) = F_+\cos 2\psi - F_\times \sin 2\psi \,, \\ F'_\times(\theta,\phi,\psi) = F_+\sin 2\psi + F_\times \cos 2\psi \,. \end{array} \tag{40}$$

When average quantities have to be computed, one has to evaluate terms like

$$\int d\Omega(\theta,\phi) F_{+,\times} F_{+,\times} \,.$$

However mixed integrals of the type $\int F_+ F_\times$ vanish as they involve an odd number of $\hat{\mathbf{u}}$ and $\hat{\mathbf{v}}$ vectors and $\hat{\mathbf{u}}$ ($\hat{\mathbf{v}}$) is odd (even) under $\hat{\mathbf{n}} \to -\hat{\mathbf{n}}$. Moreover the average of F_+^2 and $F_\times^2$ are equal (since $\int d\psi \cos 2\psi \sin 2\psi = 0$ and $\int d\psi \cos^2 2\psi = \int \sin^2 2\psi = \pi$) For an interferometer the pattern functions are

$$\begin{array}{rcl} F_+(\theta,\phi) & = & \frac{1}{2}\left(1+\cos^2\theta\right)\cos 2\phi \\ F_\times(\theta,\phi) & = & \cos\theta \sin 2\phi \end{array} \tag{41}$$

with average

$$\langle F_+^2 \rangle = \frac{1}{4\pi}\int F_+^2(\theta,\phi)\, d\cos\theta d\phi = \frac{2}{5}\,. \tag{42}$$

4 Source's order of magnitudes

Interferometric detectors are very precise and rapidly responsive ruler, they can detect the change of an arm length down to values of 10^{-15} m, however not at all frequency scales. At very low frequency ($f_{GW} \lesssim 10$ Hz) the noise from seismic activity and generic vibrations degrade the sensitivity of the instrument, whereas at high frequency laser shot noise does not allow to detect signal with frequency larger than few kHz. Considering a binary system in circular orbit, its emission depend only on one parameter according to

$$F(v) = \frac{32\eta^2}{5G_N} v^{10}\left(1 + f_{v^2}(\eta) v^2 + f_{v^3}(\eta) v^3 + \ldots\right)\,. \tag{43}$$

where $\eta \equiv m_1 m_2/M^2$, $M \equiv m_1 + m_2$) and $v \equiv (G_N M \pi f_{GW})^{1/3}$ coincide with Newtonian velocity as it can be derived by using Kepler's law for circular orbits $R^3/T^2 = G_N M/(2\pi)^2$ and remembering that $f_{GW} = 2/T$. What is the typical length, mass, radius scale of the source? Using again third's Kepler law and circular motion we have

$$\begin{array}{rlcl} V = & (G_N M \pi f_{GW})^{1/3} & \simeq & 0.054\left(\frac{M}{M_\odot}\right)^{1/3}\left(\frac{f_{GW}}{10\text{Hz}}\right)^{1/3}, \\ r = & 2G_N M (G_N M \pi f_{GW})^{-2/3} & \simeq & 6.4\text{Km}\left(\frac{M}{M_\odot}\right)^{1/3}\left(\frac{f_{GW}}{10\text{Hz}}\right)^{-2/3}. \end{array} \tag{44}$$

It can also be interesting to estimate how long it will take to for a coalescence to take place. Using the lowest order expression for energy and flux, one has

$$
\begin{aligned}
-\eta M v \frac{dv}{dt} &= -\frac{32}{5G_N}\eta^2 v^{10} \implies \\
\frac{dv}{v^9} &= \frac{32\eta}{5G_N M} dt \implies \\
\frac{1}{v_i^8} - \frac{1}{v_f^8} &= \frac{256\eta}{5G_N M}\Delta t \,,
\end{aligned}
\tag{45}
$$

for the time Δt taken for the inspiralling system to move from v_i to v_f. If $v_i \ll v_f$ we can estimate

$$
\Delta t \simeq \frac{5G_N M}{256\eta} v_i^{-8} \simeq 1.4\times 10^4 \mathrm{sec}\frac{1}{\eta}\left(\frac{M}{M_\odot}\right)^{-5/3}\left(\frac{f_{iGW}}{10Hz}\right)^{-8/3} . \tag{46}
$$

Note that v_f can be comparable to v_i for very massive systems, which enter the detector sensitivity band when $v_i \lesssim 1$. For an estimate of the maximum relative binary velocity during the inspiral, we can take the inner-most stable circular orbit v_{ISCO} of the Schwarzschild case, which gives

$$
v_{ISCO} = \frac{1}{\sqrt{6}} \simeq 0.41 \,. \tag{47}
$$

The number of cycles N the GW spends in the detector sensitivity band can be derived by noting that

$$
E = -\frac{1}{2}\eta M \left(G_N M \pi f_{GW}\right)^{2/3} \tag{48}
$$

and

$$
\begin{aligned}
\Delta N(t) &= \int_{t_i}^{t} f_{GW}(t')dt' \implies \\
N(f_{GW}) &\simeq \int_{f_{iGW}}^{f_{GW}} f\frac{dE/df}{dE/dt}df \\
&\simeq \frac{5G_N M}{96\eta}\int_{f_{iGW}}^{f_{GW}} \left(G_N M\pi f\right)^{-8/3} df \\
&= \frac{1}{32\pi\eta}\left(G_N M\pi\right)^{-5/3}\left(\frac{1}{f_{iGW}^{-5/3}} - \frac{1}{f_{GW}^{-5/3}}\right) \\
&\simeq 1.5\times 10^5 \frac{1}{\eta}\left(\frac{M}{M_\odot}\right)^{-5/3}\left(\frac{f_{iGW}}{10\mathrm{Hz}}\right)^{-5/3}
\end{aligned}
\tag{49}
$$

We can finally obtain the time evolution of the GW frequency

$$
\dot{f}_{GW} = \frac{96}{5}\pi^{8/3}\eta\left(G_N M\right)^{5/3} f_{GW}^{11/3} \tag{50}
$$

which has solution

$$
\begin{aligned}
f_{GW}(t) &= \frac{1}{\eta^{3/8}\pi}\left(\frac{5}{256}\frac{1}{|t-t_{coa}|}\right)^{3/8} G_N M^{-5/8} \\
&= 151\mathrm{Hz}\frac{1}{\eta^{3/8}}\left(\frac{M}{M_\odot}\right)^{-5/8}\left(\frac{|t|}{1\mathrm{sec}}\right)^{-3/8} ,
\end{aligned}
\tag{51}
$$

which can be inverted to give

$$|t - t_{coa}| = \frac{5G_N M}{256\pi\eta}\left(\frac{1}{\pi G_N M f_{GW}}\right)^{5/3} . \tag{52}$$

The typical GW strain at the detector from a binary source is

$$h \sim \frac{2G_N \mu v^2}{d} \sim 10^{-22}\left(\frac{\mu}{M_\odot}\right)\left(\frac{v}{0.1}\right)^2\left(\frac{d}{Mpc}\right)^{-1} \tag{53}$$

5 An example: a specific waveform from binary inspiral

Starting from the GW expression in term of the source quadrupole

$$h_{ij}^{TT}(t, \mathbf{x}) = \frac{2G_N}{d}\Lambda_{ij;kl}(\hat{\mathbf{n}})\ddot{M}_{kl}(t) \tag{54}$$

For $\hat{\mathbf{n}} = \hat{\mathbf{z}}$

$$\Lambda_{ij;kl}M_{kl} = \begin{pmatrix} (M_{xx} - M_{yy})/2 & M_{12} & 0 \\ M_{12} & (M_{yy} - M_{xx})/2 & 0 \\ 0 & 0 & 0 \end{pmatrix} \tag{55}$$

we have

$$\begin{aligned} h_+ &= G_N \frac{\ddot{M}_{xx} - \ddot{M}_{yy}}{d} , \\ h_+ &= \frac{2G_N \ddot{M}_{xy}}{d} . \end{aligned} \tag{56}$$

Assuming the sources are in circular motion, their relative distance can be parametrized as for

$$\begin{aligned} x(t) &= r\sin(\omega_s t) , \\ y(t) &= -r\cos(\omega_s t) , \\ z(t) &= 0 , \end{aligned} \tag{57}$$

hence yielding to

$$\begin{aligned} \ddot{M}_{xx} &= -\ddot{M}_{yy} = 2\mu r^2 \omega_S^2 \cos(2\omega_s t) \\ \ddot{M}_{xy} &= 2\mu r^2 \omega_S^2 \sin(2\omega_s t) \end{aligned} \tag{58}$$

When the orbital planes is inclined by an angle ι with respect to the propagation direction (conventionally kept along the z-axis) one has to compute the rotated projected quadrupole tensor according to

$$M'_{ij} = R^{(y)}(\iota)_{ii'} M_{i'j'} \left(R^{(y)}\right)^{-1}_{j'j}(\iota) \tag{59}$$

and then project it with Λ to obtain

$$\Lambda_{ij,kl}M'_{kl} = \begin{pmatrix} \cos^2\iota M_{xx}/2 - M_{yy}/2 & \cos\iota M_{xy} & 0 \\ \cos\iota M_{xy} & M_{yy}/2 - \cos^2\iota M_{xx}/2 & 0 \\ 0 & 0 & 0 \end{pmatrix} . \tag{60}$$

Now using the explicit expressions eqs. (58) one finds

$$\begin{aligned} h_+ &= \frac{1}{d} 4 G_N \mu \omega_S^2 R^2 \left(\frac{1+\cos^2\iota}{2}\right)\cos(2\omega_s t)\,, \\ h_\times &= \frac{1}{d} 4 G_N \mu \omega_S^2 R^2 \cos\iota \sin(2\omega_s t)\,. \end{aligned} \tag{61}$$

Note that the rotation (59) is not the most generic rotation setting the orbital plane at an angle ι with the view direction $(0,0,1)$: an additional rotation by ψ around the z axis is permitted. However this is not an additional degree of freedom with respect to the polarization angle ψ introduced in eq. (40) as it corresponds to a common rotation of the $\hat{\mathbf{u}}$ and $\hat{\mathbf{v}}$ vector in the orbital plane.

Using $f_{GW} = \omega_s/\pi$ and the explicit expression $f_{GW}(t)$ eq. (51) one has

$$\begin{aligned} h_+(t) &= \frac{1}{d}\left(G_N M_c\right)^{5/4}\left(\frac{5}{\tau}\right)^{1/4}\left(\frac{1+\cos^2\iota}{2}\right)\cos\Phi(\tau) \\ h_\times(t) &= \frac{1}{d}\left(G_N M_c\right)^{5/4}\left(\frac{5}{\tau}\right)^{1/4}(\cos\iota)\sin\Phi(\tau) \end{aligned} \tag{62}$$

For data analysis we actually need this expression in frequency space, so let us compute it for the + polarization

$$\tilde{h}_+(f) = \frac{1}{2}\int dt A(t)\left(e^{i(2\pi f t + \Phi(\tau(t)))} + e^{i(2\pi f t - \Phi(\tau(t)))}\right)\,, \tag{63}$$

where $A(t)$ is defined by comparison with the (62). The above integral can be computed in the *stationary phase approximation* by expanding the exponent in the integrand around the stationary point t_* characterized by

$$2\pi f - \dot{\Phi}(\tau(t_*)) = 2\pi f + \left.\frac{d\Phi(\tau)}{d\tau}\right|_{\tau=t_c-t_*} = 0 \tag{64}$$

as follows:

$$e^{2\pi i f t - i\Phi(t)} \to e^{2\pi i f t_* - i\Phi(t_*)}\exp\left(-i\ddot{\Phi}(t_*)\frac{(t-t_*)^2}{2}\right) \tag{65}$$

then performing the resulting Gaussian integral as

$$\begin{aligned} \tilde{h}_+(f) &= \frac{1}{2}A(t_*)e^{i(2\pi f t_* - \Phi(t_*))}\int dt\, e^{-i\ddot{\Phi}(t_*)(t-t_*)^2/2} \\ &= \frac{1}{2}A(t_*)e^{i(2\pi f t_* - \Phi(t_*) - \pi/4)}\left(\frac{2\pi}{\ddot{\Phi}(t_*)}\right)^{1/2}\,. \end{aligned} \tag{66}$$

Time t_* can be expressed in terms of f_{GW} by inverting (51) and eq. (64) enable the identification between the Fourier transform argument f and f_{GW}, thus allowing to write

$$\tilde{h}_+(t_*(f)) = \left(\frac{5}{24}\right)^{1/2}\frac{\pi^{-2/3}}{d}(G_N M_c)^{5/6} f^{-7/6}\left(\frac{1+\cos^2\theta}{2}\right)e^{i(2\pi i t_* f - \Phi(t_*) - \pi/4)}\,. \tag{67}$$

It is useful to introduce

$$v \equiv (\pi G_N M f_{GW})^{1/3} = (G_N M\omega)^{1/3}\,. \tag{68}$$

The most commonly used approximant is defined in the frequency domain as *TaylorF2*:

$$\begin{aligned}
\psi(f) &= 2\pi f t_* + \phi_{ref} - 2\int^f \omega \frac{dt}{df} df \\
&= \phi_{ref} + \frac{2}{G_N M}\int^f (v_f^3 - v^3(f'))\frac{v(f')}{f'}\frac{dE/dv}{dE/dt}\frac{f'}{v(f')}\frac{dv}{df'}df' \\
&= 2\pi \int^f (v_f^3 v^{-2} - v)\left[\frac{-\eta M v}{-32/(G_N 5)\eta^2 v^{10}}\right]\frac{1}{3}df' \\
&= \frac{5\pi G_N M}{48\eta}\int^f (v_f^3 v^{-11} - v^{-8})\left(1 + c_{1PN}v^2 + \ldots\right) df' \\
&= \frac{5}{48\eta}(\pi G_N M f)^{-8/3}\left[\left(-\frac{3}{8}+\frac{3}{5}\right) + \left(-\frac{1}{2}+1\right)c_{1PN}\ldots\right] \\
&= \frac{3}{128\eta v^5(f)}\left(1 + \frac{20}{9}c_{1PN}v^2(f) + \ldots\right)
\end{aligned} \tag{69}$$

It may also be useful to have an expression of the phase in time-domain. Let us now relate the phase of the waveform to the dynamics of the sources by defining

$$\begin{aligned}
\Delta\phi(t) &= 2\pi\int_{t_0}^t f_{GW}(t')dt' = 2\int_{v(t_0)}^{v(t)} \omega(v)\frac{dE/dv}{dE/dt}dv \\
&= \frac{2}{G_N M}\int_{v(t_0)}^{v(t)} v^3 \frac{dE/dv}{dE/dt}dv \\
&= \frac{5}{16\eta}\int_{v(t_0)}^{v(t)} \frac{1}{v^6}\frac{1 + e_{v^2}v^2 + \ldots}{1 + f_{v^3}v^3 + f_{v^4}v^4 + \ldots}dv\,,
\end{aligned} \tag{70}$$

where we have inserted the formal Taylor expansion of the energy and flux as functions of v and we have substituted $v = (G_N M\omega)^{1/3}$ (that is valid for circular orbits). We now see that we have different possibilities to compute the phase

- Truncate the v-series at some order both in the numerator and the denominator gives rise to the *TaylorT1* expression of the phase
- Expand the fraction in the above formula and truncate at some finite v-order $\to$ *TaylorT4*
- expand the inverse of the fraction appearing in the integrand $\to$ *TaylorT1*.

6 Elements of data analysis

The output of the detector $o(t)$ is a scalar time domain function, which in general will result of the addition of a part $h(t)$ linear in the impinging GW $h_{ij}(t, \mathbf{x}_D)$

at the location detector $\mathbf{x}_D$ and the instrumental noise $n(t)$. Usually the output of the detector is linearly related to the GW amplitude locally in the frequency space, i.e.

$$\tilde{h}(f) = \tilde{T}_{ij}(f)\tilde{h}_{ij}(f) \tag{71}$$

where $T_{ij}(f)$ is the *transfer function* of the system and

$$\tilde{o}(f) = \tilde{h}(f) + \tilde{n}(f)\,. \tag{72}$$

If the noise is *stationary* then different Fourier components are uncorrelated (see derivation below) and we can write

$$\langle \tilde{n}^*(f)\tilde{n}(f')\rangle = \delta(f-f')\frac{1}{2}S_n(f)\,, \tag{73}$$

which defines the *noise correlation function* $S_n(f)$, or *noise power spectral density*, with dimensions Hz^{-1}. Note also that $S_n(-f) = S_n(f)$.

The average in eq. (73) is taken over many noise realizations, but we have only one detectors, so it should be actually replaced over different time span averages:

$$\langle \tilde{n}^*(f)\tilde{n}(f')\rangle = \frac{1}{N}\sum_{i=1}^{N}\tilde{n}_i(f)\tilde{n}_i^*(f')\,,$$

where

$$\tilde{n}_i(f) = \int_{t_i-T/2}^{t_i+T/2} n(t)e^{2\pi i f t}dt\,,$$

and $t_i = (\ldots,-2T,-T,0,T,2T,\ldots)$. We define the Fourier Transform of a function defined on an interval as

$$\tilde{n}(f) = \int_{t_i-T/2}^{t_i+T/2} n(t)e^{2\pi i f t}\,dt \qquad \text{with } n(t+T)=n(t) \tag{74}$$

with the periodicity requirement implying the Fourier transform $\tilde{n}(f)$ be discrete, with support at $f_n = n/T$, i.e. with frequency resolution $\Delta f = 1/T$. This discreteness condition on the frequency automatically ensure that the inverse Fourier transform returns a periodic function[2]:

$$n(t) = \frac{1}{T}\sum_{n\in\mathbb{N}}\tilde{n}(f)e^{-2\pi i n t/T}\,. \tag{76}$$

---

[2]Note that the definition (74) for a function defined on an interval is *not* equivalent to

$$\tilde{n}(f) \neq \int_{-\infty}^{\infty} n(t)e^{2\pi i f t}\theta(t-t_i+T/2)\theta(t_i+T/2-t)dt\,.$$

Had we used this definition one would have dealt with a non-analytic integrand in the time integral, that would have had discontinuities in his derivatives. As the discontinuities in the direct space functions are related to "bad" behaviour at infinity via

$$\frac{d^m n(t)}{dt^m} = \int df(2\pi i f)^m\tilde{n}(f)e^{2\pi i f t} \tag{75}$$

one would expect in general a non-physical high power in $\tilde{n}(f)$ for large $|f|$, or that $f^m\tilde{n}(f)$ must not be integrable, that is $\lim_{f\to\infty}|f^{m+1}n(f)|^2 \neq 0$. It is a general rule that the the large f behaviour of $\tilde{n}(f)$ depends on the continuity property of $n(t)$.

A very welcome by-product of the definition (74), restricting the integration domain to a finite interval and imposing periodicity condition on $n(t)$, is

$$\frac{1}{T}\int_{t_i-T/2}^{t_i+T/2} e^{2i\pi ft}dt = \frac{e^{2i\pi ft_i}}{2\pi ifT}\left(e^{2\pi ifT/2} - e^{-2\pi ifT/2}\right) = e^{2\pi ift_i}\frac{\sin(\pi fT)}{\pi fT} = \delta_{f,0} \tag{77}$$

which is reminiscent of the standard $\int e^{2i\pi ft}dt = \delta(f)$ valid for functions defined on the entire real axis. The only difference between the finite segment and the entire real axis case is that here we deal with a dimension-less, discrete Kronecker delta rather than a delta function with dimension of time, so that the identification

$$\delta(f) \to T\delta_{f,0} \tag{78}$$

can be made.

Let us consider than the definition (73) and exploit the stationarity property of the noise:

$$\begin{aligned}
\langle\tilde{n}(f)\tilde{n}(f')\rangle &= \int_{-T/2}^{T/2} dt \int_{-T/2}^{T/2} dt' \langle n(t)n(t')\rangle e^{2\pi i(ft+f't')} \\
&= \int_{-T/2}^{T/2} dt \int_{-T/2}^{T/2} dt' \langle n(t+T_s)n(t'+T_s)\rangle e^{2\pi i(ft+f't'+T_s(f+f'))} \\
&= \delta_{f+f',0}\int_{-T/2}^{T/2}\int_{-T/2}^{T/2} \langle n(t)n(t')\rangle e^{2\pi if(t-t')}
\end{aligned} \tag{79}$$

where we have averaged over a time coordinate T_s and used stationarity to substitute $n(t+T_s) \to n(t)$ inside the average. Short-circuiting the above with the definition (73) and the correspondence (78) we obtain

$$S(f) = 2\frac{\langle|\tilde{n}(f)|^2\rangle}{T} = 2\langle|\tilde{n}(f)|^2\rangle\Delta f\,. \tag{80}$$

We can make the further connection to the noise auto-correlation function

$$R(\tau) \equiv \langle n(t+\tau)n(t)\rangle\,, \tag{81}$$

white noise corresponding to $R(\tau) \propto \delta(\tau)$. By noting that

$$\begin{aligned}
&\langle\int df' \int df\, n(f)n(f')e^{-2\pi i(f(t+\tau)+f't)}\rangle \\
=\ &\frac{1}{2}\int df S_n(f)e^{-2\pi if\tau}
\end{aligned} \tag{82}$$

we are enabled to interpret the noise spectral density function as the Fourier transform of the noise correlation function

$$\frac{1}{2}S_n(f) = \int d\tau R(\tau)e^{2\pi if\tau} \tag{83}$$

and hence

$$R(\tau) = \frac{1}{T} \sum_{n \in \mathbb{N}} e^{-2\pi i f \tau} \frac{S_n(f)}{2} \, . \tag{84}$$

The factor 1/2 in the definition is conventionally inserted as

$$\begin{aligned} \langle n^2(t) \rangle &= \frac{1}{T^2} \sum_n \sum_{n'} \langle n(f) n(f') \rangle e^{2\pi i (ft + f't')} \\ &= \frac{1}{2T} \sum_{n \in \mathbb{N}} S_n(f) = \frac{1}{T} \sum_{n \geq 0} S_n(f) \end{aligned} \tag{85}$$

and the factor 1/2 disappears when sum is taken over positive frequencies only (we neglect subtleties about the $n = 0$ mode). The power spectral density of white noise is f-independent.

Actually in practice the time domain noise function will be discrete as well, implying that what we'll be really using are

$$\begin{aligned} \tilde{n}(f = k/T) &= \Delta t \sum_{j=0}^{N-1} e^{2\pi i j k \Delta t / T} \\ n(t = j\Delta t) &= \Delta f \sum_{j=0}^{N-1} e^{2\pi i j k \Delta t / T} \end{aligned} \tag{86}$$

with $\Delta f \Delta t = 1/N$ with $T/\Delta t = N$. With a finite sampling size there has to be a maximum frequency, called the *Nyquist frequency*

$$f_{Nyquist} = \frac{1}{2\Delta t} \tag{87}$$

so that we have N points for $n(t)$ and $N/2 + 1$ for $\tilde{n}(f)$ if N is even, as we will assume. Note that $\tilde{n}(f = 0)$ is real as well as $n(f = N/(2T))$ so that the information stored in the N real numbers of $n(t)$ is fully equivalent to the information stored in the $N/2 + 1$ numbers making up $\tilde{n}(f)$, 2 of which are real and $N/2 - 1$ of which are complex.

In particular the Parseval identity has a discrete counterpart

$$\Delta f \sum_{k=0}^{N/2} |\tilde{n}(k/T)|^2 = \Delta t \sum_{j=0}^{N-1} n^2 (j\Delta t) \, . \tag{88}$$

6.1 Matched filtering

The signal amplitude is much smaller than the noise, just think of the earth gravitational field that is responsible for $h \sim 10^{-9} \gg 10^{-21}$. However if the signal is known in advance, we can correlate detector's output $o(t)$ with our expectation and dig it out of the noise floor. We thus have to *filter* the detector output to highlight the signal. An important quantity for any experiment is the *signal-to-noise ratio (SNR)* we are going to define now. It must involve a ratio

S/N of a quantity linear in the signal h possibly filtered in order to enhance it and a quantity representative of the noise. We want to choose the filter function so to maximize the SNR, i.e. the filter has to *match* the signal. We can assume that by linearly filtering the detector output we can pick only the signal part $h(t)$ in $o(t)$ and we can tentatively define the numerator of the SNR as

$$S = \int dt \langle o(t) \rangle K(t)\,, \tag{89}$$

and since $\langle n(t) \rangle = 0$ we have

$$S = \int dt \langle h(t) \rangle K(t) = \int df \tilde{h}(f) \tilde{K}^*(f)\,, \tag{90}$$

where for simplicity we have moved back to continuum time-frequency space. For the SNR denominator N we want an estimator of the noise. A reasonable guess would be the root mean square of the detector output in absence of the signal, i.e.

$$N^2 \stackrel{?}{=} \langle o^2(t) \rangle - \langle o(t) \rangle^2|_{h=0} = \langle n(t) \rangle^2 \tag{91}$$

but we want the overall filter scale to drop out of the SNR, so we'd better define

$$\begin{aligned} N^2 &= \int dt\, dt'\, K(t)K(t') \langle n(t)n(t') \rangle \\ &= \int df\, df' \langle n(f)n(f') \rangle e^{2\pi i(ft+ft')} \tilde{K}(f)\tilde{K}(f') \\ &= \frac{1}{2} \int df S_n(f) |\tilde{K}(f)|^2\,. \end{aligned} \tag{92}$$

We have constructed then our SNR as

$$\frac{S}{N} = \frac{2 \int df \tilde{h}(f) \tilde{K}^*(f)}{\int df S_n(f) |\tilde{K}(f)|^2}\,. \tag{93}$$

In order to find the filter function maximizing the SNR we define a positive definite scalar product

$$(A|B) \equiv 2 \int df \frac{A(f)B^*(f)}{S_n(f)} \tag{94}$$

which is real if we assume that $A^*(f) = A(-f)$ and $B^*(f) = B(-f)$, as it is for the Fourier transform of real functions. We can now re-write the SNR as

$$\frac{S}{N} = \frac{(\tilde{u}|\tilde{h})}{(\tilde{u}|\tilde{u})^{1/2}} \tag{95}$$

with $\tilde{u}(f) \equiv 1/2 S_n(f) \tilde{K}(f)$. We are thus searching for the normalized vector u that maximizes its scalar product with h, clearly the solution can only be $\tilde{u} \propto \tilde{h}$, i.e.

$$\tilde{K}(f) = \frac{\tilde{h}(f)}{S_n(f)} \tag{96}$$

up to an inessential f-independent constant. Substituting in eq. (93) we finally obtain

$$\frac{S}{N} = \left[2 \int_{-\infty}^{\infty} df \, \frac{|\tilde{h}(f)|^2}{S_n(f)} \right]^{1/2} . \tag{97}$$

So far we have assumed perfect knowledge of the signal. What if we do not know the exact *time location* of the $h(t)$? By considering a function $h(t)$ and its time-shifted $h_{t_0}(t) \equiv h(t-t_0)$ the relationship among their Fourier transform is

$$\tilde{h}(f) = \tilde{h}_{t_0}(f) \, e^{2\pi i f t_0} . \tag{98}$$

If we try to match data $\tilde{h}(f)$ with a *template* signal $\tilde{h}_{tmplt}(f)$ allowing for a generic time-shift t, we obtain an SNR time series

$$\begin{aligned} SNR(t) &= \sqrt{2} \frac{\int_{-\infty}^{\infty} df \, \frac{\tilde{h}(f)\tilde{h}^*_{tmplt}(f)}{S_n(f)} e^{2\pi i f t}}{\left(\int_{-\infty}^{\infty} df \, |\tilde{h}_{tmplt}(f)|^2 / S_n(f) \right)^{1/2}} = \\ &= \frac{\int_0^{\infty} df \, \left(\tilde{h}(f)\tilde{h}^*_{tmplt}(f) + \tilde{h}^*(f)\tilde{h}_{tmplt}(f) \right) e^{2\pi i f t} / S_n(f)}{\left(\int_0^{\infty} df \, |\tilde{h}_{tmplt}(f)|^2 / S_n(f) \right)^{1/2}} \end{aligned} \tag{99}$$

and the use of a Fast Fourier Transform allows to search for all time values efficiently.

Let us consider now the case of a constant phase offset between the template and the signal and let us concentrate on the simplified situation of a signal $h(t) \propto \cos(2\pi f_0 t)$, i.e. $\tilde{h}(f) \propto \delta(f - f_0) + \delta(f + f_0)$.
Taking the correlator with a filter function of the type $K(t) \propto \cos(2\pi f_1 t + \bar{\phi})$ we would have a non-null result in case $f_0 = f_1$ proportional to $\cos(\phi)$. Clearly the filter *is* matching the signal but our ignorance on the right ϕ value may suppress the matched filter output. What one would like is the SNR time series to be the maximum as $\bar{\phi}$ varies. It turns out that it is in fact possible to maximize over $\bar{\phi}$ analytically. In order to show how let us fix the $t = 0$ for simplicity:

$$\begin{aligned} \frac{S}{N}(t=0) &= \int_{-\infty}^{\infty} \tilde{h}(f)\tilde{K}(-f)e^{-i\bar{\phi}} df \\ &= \int_0^{\infty} \left(\tilde{h}(f)K(-f)e^{i\bar{\phi}} + \tilde{h}(-f)K(f)e^{-i\bar{\phi}} \right) df = \\ &= \mathcal{R}\cos\bar{\phi} + \mathcal{I}\sin\bar{\phi} , \end{aligned} \tag{100}$$

where the real quantities $\mathcal{R}$ and $\mathcal{I}$ are defined as

$$\begin{aligned} \mathcal{R} &\equiv \int_0^{\infty} \left(\tilde{h}(f)\tilde{K}^*(f) + \tilde{h}^*(f)\tilde{K}^*(f) \right) df &&= 2Re \int_0^{\infty} \tilde{h}(f)\tilde{K}(f) df \\ \mathcal{I} &\equiv -i \int_0^{\infty} \left(h(f)K^*(f) - h^*(f)K(f) \right) df &&= 2Im \int_0^{\infty} \tilde{h}(f)\tilde{K}^*(f) df . \end{aligned} \tag{101}$$

The output of the matched filter depends on $\bar{\phi}$, but analytically maximizing over $\bar{\phi}$ is possible:

$$\frac{dS/N}{d\phi_0} = 0 \implies \cos\bar{\phi} = \frac{\mathcal{R}}{\sqrt{\mathcal{R}^2+\mathcal{I}^2}}\,, \qquad \sin\bar{\phi} = -\frac{\mathcal{I}}{\sqrt{\mathcal{R}^2+\mathcal{I}^2}}\,, \tag{102}$$

which give the SNR maximized over $\bar{\phi}$

$$\overset{Max}{\phi_0} \left(\frac{S}{N}\right)^2\Bigg|_{t=0} = \mathcal{R}^2 + \mathcal{I}^2\,. \tag{103}$$

Note that there is an efficient way to compute both the quantities $\mathcal{R}$ and $\mathcal{I}$: it is by computing the *complex inverse Fourier transform*

$$\rho(t) \equiv \sqrt{2}(\tilde{h}_{tmplt}|\tilde{h}_{tmplt})^{-1/2}\int_0^\infty \frac{\tilde{h}(f)\tilde{h}_t^*(f)}{S_n(f)}e^{2\pi i f t}df \tag{104}$$

and we have

$$\overset{Max}{\phi_0}\,\frac{S}{N}(t) = 2\sqrt{2}|\rho(t)|\,. \tag{105}$$

Templates differing by a phase shift like $\tilde{h}_{tmplt}(f) \to \tilde{h}'_{tmplt}(f) = \tilde{h}_{tmplt}(f)e^{i\phi_0}$ (for $f > 0$ and $\tilde{h}'_{tmplt}(f) = \tilde{h}_{tmplt}(f)e^{-i\phi_0}$ for $f < 0$) will give rise to different SNRs, but the modulus of ρ obtained with them will be the same.

7 False alarms, false dismissals and receiver operating characteristics

Let us consider the phase-maximized SNR time-series, i.e. $|\rho(t)|$. We can decide to define a candidate trigger any data chunk around an instant of time when it exceeds a given threshold.

If the detector noise is Gaussian both $Re(\rho)$ and $Im(\rho)$ are Gaussian random variables so $R \equiv \rho^2$ is a chisq distributed with 2 degrees of freedom (aka *Rayleigh* distribution) random variable

$$p(R|h=0)dR = \frac{1}{2\pi}\int_0^{2\pi}\frac{d\theta}{2\pi}\frac{dR}{2}e^{-R/2}\,, \tag{106}$$

where we have used that ρ has unit variance.

In the presence of a signal both $Re(\rho)$ and $Im(\rho)$ will have an expected non-zero value, say $\bar{x}$ and $\bar{y}$, such that $\bar{R} \equiv \bar{x}^2 + \bar{y}^2$. Then the R distribution will be:

$$p(R|\bar{R}) \propto \int_0^{2\pi}\frac{d\theta}{2\pi}\int_{-\infty}^{\infty} d\bar{x}d\bar{y}\delta(\bar{R}-(\bar{x}^2+\bar{y}^2))e^{-[(x-\bar{x})^2+(y-\bar{y})^2]/2}\frac{dR}{2} \tag{107}$$

where $x = R\cos\theta$, $y = R\cos\theta$. The integral is performed by substituting $\bar{x} \equiv r\cos\theta'$, $\bar{y} \equiv r\sin\theta'$, then getting an integral in $\alpha \equiv \theta - \theta'$ which give rise to the final result

$$\begin{aligned} P(R|\bar{R}) &\propto e^{-(R+\bar{R})/2}\int_0^{2\pi} e^{\sqrt{R\bar{R}}\cos\alpha} d\alpha \\ &= \frac{1}{2}e^{-(R+\bar{R})/2} I_0(\sqrt{R\bar{R}}) \end{aligned} \tag{108}$$

where $I_0(x) = J_0(ix)$ is the modified Bessel function ($J_0(x)$ is the standard Bessel function of the first kind). The mean and variance of R are given by

$$\begin{aligned} \langle R\rangle &= \int_0^\infty dRRP(R|\bar{R}) &= 1+\bar{R}\,, \\ \langle R^2\rangle &= \int_0^\infty dRR^2P(R|\bar{R}) &= 3+6\bar{R}+6\bar{R}^2\,. \end{aligned} \tag{109}$$

Given the distribution of the maximized SNR in the absence of a signal, what is the probability of having a *false alarm* p_{FA}, i.e. that a large noise fluctuation will be traded for a fake signal? It depends on the threshold R_t we set for event triggers:

$$p_{FA} \equiv \int_{R_t}^\infty P(R|R_h = 0) = \frac{1}{2}\int_{R_t}^\infty e^{-R/2}dR\,. \tag{110}$$

Deciding what is the maximum false alarm rate that one is willing to tolerate determine R_t, as p_{FA} is a monotonically decreasing function of R_h. This value can now be fed in the pdf of the maximized SNR-squared (108) to determine what is the corresponding *efficiency* η for a given signal strength $\bar{R}$:

$$\eta \equiv \int_{R_t}^\infty p(R|\bar{R}) \tag{111}$$

that quantifies the probability that a signal with $SNR > R_t$ is actually detected and which is a monotonically decreasing function of R_t for any given R_h. A useful concept to introduce is then the the *Receiver Operating Characteristic* (ROC) of a detector, which is the curve obtained by plotting η vs. p_{FA}, which is a monotonically increasing curve passing for the origin [3]. Picking a point on the ROC curve determines the working point of the experimental device.

Sometimes in literature it is also mentioned the complementary quantity to the efficiency, which is the *false dismissal probability* p_{FD}

$$p_{FD} \equiv 1-\eta = \int_0^{R_t} p(R|R_h)dR \tag{112}$$

Most of the material of these notes is taken from *Gravitational Waves*, Oxford University Press 2008, by Michele Maggiore.

[3] Once the background rate of a detector is known, by multiplying it by p_{FA} the false alarm rate is derived, so it is possible to build a ROC curve by plotting η vs. false alarm rate.

References

[1] F. Pirani, *Measurements of Classical Gravitation Fields*, in "The role of Gravitation in Physics", C. M. DeWitt and D. Rickles eds., proceedings of the 1957 Chapel Hill Conference, Max Planck Research Library for the History and Development of Knowledge.

[2] J. B. Hartle, "Gravity. An introduction to Einstein's General Relativity". Addison Wesley, S. Franscisco (2003).

[3] A. Freise and K. A. Strain, "Interferometer Techniques for Gravitational-Wave Detection", Living Rev. Relativity 13, (2010), 1. URL: http://www.livingreviews.org/lrr-2010-1

[4] M. Maggiore, "Gravitational Waves". Oxford University Press, Oxford (2008).

[5] P. R. Saulson, "How an interferometer extracts and amplifies power from a gravitational wave," Class. Quant. Grav. **14** (1997) 2435.

[6] J. Hough, In *Perth 1988, Proceedings, Recent developments in theoretical and experimental general relativity, gravitation and relativistic field theories, pt. A* 265-282.